Photodissociation dynamics of H_2S isolated in krypton matrices

J. Zoval, D. Imre, P. Ashjian and V.A. Apkarian [1]

Department of Chemistry, Institute for Surface and Interface Science, University of California, Irvine, CA 92717, USA

Received 28 May 1992; in final form 9 July 1992

Photodissociation of H_2S in krypton matrices is followed by monitoring laser-induced fluorescence from the SH photofragment. No evidence of an energy threshold for dissociation is observed. Quantum yields of dissociation, referenced to gas-phase absorption cross sections, increase nearly linearly from 0.04 ± 0.01 to 0.25 ± 0.08, in the spectral range between 266 and 193 nm (excess energies of 0.75–2.5 eV). In addition to the SH+H direct dissociation channel, production of S atoms is observed. The latter channel is ascribed to secondary, in-cage collisions between the SH and H fragments to produce $S+H_2$.

1. Introduction

As one of the simplest prototypes of condensed phase reactive dynamics, the photodissociation of hydrides in rare-gas solids has been the focus of both experimental and theoretical studies in recent years [1–11]. The photodissociation of HI in crystalline xenon was the first system considered [1–4]. Classical molecular dynamics simulations of this system revealed that the cage exit of the H photofragment is significantly *delayed*, 1–3 ps, and proceeds after extensive thermalization by collisions with the immediate cage [1]. Mixed quantum/classical simulations, in which the H atom is treated as a quantum particle, did not change this aspect of the dynamics [2]. Extensive experimental studies on the HI/Xe system have yielded fragmentary information in support of the model [3,4]. These experiments have been complicated by interferences from previously unsuspected ionic dynamics [4]. It is now clear that in the case of al hydrogen halides isolated in heavy rare-gas solids, Xe and Kr in particular, charge separation and trapping proceeds very efficiently. The resulting charged centers are strong chromophores, therefore, ionic photoprocesses mask the neutral photodissociation dynamics [4,5]. In related studies, in a series of experimental investigations, Schwentner et al. detailed the photodissociation of H_2O/D_2O in rare-gas solids [6–10]. A major highlight of these studies was the observation of energetic thresholds to photodissociation; suggesting that: dissociation is controlled by cage exit of the H atom, and that this process is better described as a *sudden* crossing of a cage barrier which is *potential* in nature. The H_2O data were therefore interpreted in a picture which was in sharp contradiction with the delayed cage exit scenario derived from the HI studies. More recent MD simulations, and statistical calculations for sudden cage exit have failed to reproduce the conclusions derived from the H_2O experiments [11]. The present investigations on H_2S were in part prompted by these discrepancies.

The photodissociation of H_2S has been the subject of extensive theory [12–16] and experimentation [17–23] in the gas phase. Two electronic surfaces, $^1A_2$, $^1B_1$, are nested in the first absorption continuum, and cross in the Franck–Condon region. Away from the C_{2v} geometry of the ground state, in the C_s geometry, both surfaces have $^1A''$ symmetry. As such, they are not allowed to cross, but remain strongly coupled [12]. The absorption spectra can be satisfactorily simulated with the assumption of absorption to two adiabatically coupled surfaces: one purely dissociative along the HS–H coordinate, $1\,^1A''$, and the other, $2\,^1A''$, purely bound but predissociative

Correspondence to: V.A. Apkarian, Department of Chemistry, Institute for Surface and Interface Science, University of California, Irvine, CA 92717, USA.

[1] Alfred P. Sloan Fellow.

[13,16]. Resonance Raman studies indicate a dynamic interplay between these two surfaces [15], nevertheless dissociation appears to be prompt throughout the first absorption continuum [15–23]. This situation is quite different from that of H_2O in which the equivalent excited electronic surfaces are well separated energetically, and the first absorption leads to a purely dissociative surface [24]. This is an important difference between H_2S and H_2O, and one that should be kept in mind in comparing the solid-state data.

Inhibition of direct dissociation by the solid lattice, and promotion of recombination, is the classical definition of the cage effect [25]. While in the case of diatomics, recombination is the only observable cage effect, in the case of triatomics (polyatomics) new reactive channels can be promoted by the caging of photofragments. Caging of the hot SH and H photofragments can in principle promote the indirect $S(^3P, ^1D, ^1S)+H_2$ channel, where such channels are energetically accessible. Evidence for this cage-induced reaction is obtained in the present by observation of the photoproduction of atomic sulfur – both by direct laser-induced fluorescence from $S(^1S \rightarrow ^1D)$, or via S_2 thermoluminescence. The branching ratio between the two dissociation channels is now being studied. here we limit the discussion to studies in which the photodissociation of H_2S is followed by laser-induced fluorescence from the $SH(A \rightarrow X)$ photoproduct, the spectroscopy of which in solid Ar and Kr was recently reported [26]. Note, these measurements yield the overall photodissociation probability of H_2S. The available data on H_2O dissociation in matrices were obtained by monitoring the photoproduction of OH radicals (photoproduction of H has also been followed in Xe [10]), and as such pertain to overall dissociation quantum yields as well. A direct comparison of these measurements is therefore meaningful. The main result to be presented in this report is that: in contrast with the case of matrix-isolated H_2O, no energetic threshold for dissociation is observed in the case of H_2S. The absence of an energetic dissociation threshold would be in agreement with the MD simulations, which predict cage exit only after extensive thermalization.

2. Experimental

It is most desirable to carry out these photodynamical studies in solids of known morphology. Ideally, isolation of the molecule in a crystalline lattice is sought. As such, a significant effort was expended to trap H_2S in free standing crystals of Ar and Kr, which provide longer range crystallinity than matrices. Even at dilutions of 10000:1, H_2S aggregates in Ar, as in the recently reported case of N_2O [27]. In free standing crystals of Kr, dimerization of H_2S could not be prevented. This was verified by infrared studies, and the photoproduction of S_2 which could be followed by its intense $B \rightarrow X$ fluorescence [28,29]. The relative intensity of SH versus S_2 laser-induced fluorescence was subsequently used as a guideline for the extent of isolation of H_2S in different media. The infrared absorption of H_2S doped crystalline Kr, dominated by dimer absorptions, is shown in the inset to fig. 1. The fluorescence spectrum of SH excited on the $A(v=1) \leftarrow X(v=0)$ transition at 311 nm [22], and S_2 excited on the $B(^3\Sigma_u^-, v=3) \leftarrow X(^3\Sigma_g^-, v=0)$ transition in the same crystal are shown in fig. 1, on the same absolute scale. The S_2 absorption coefficient and quantum yield of emission is expected to be significantly smaller than that of SH in this range, however the fluorescence intensities are comparable. Due to this extensive dimerization, free standing crystals were abandoned for the dynamical studies. However, due to the advantages of high optical quality and long pathlength, absorption spectra were recorded in such a crystal at an estimated dilution of 1:100000. In the spectral range of 200–280 nm (short wavelength limit dictated by the operating range of the spectrometer), the band profile closely agrees with the gas-phase spectrum of H_2S which was also recorded on the same instrument.

The photodissociation measurements were conducted in matrices prepared by pulsed deposition. At dilutions of 1:10000, no evidence for S_2 formation with UV irradiation was found. Based on the detection sensitivities used, it is possible to assert that the dimer concentration in the matrix was four orders of magnitude less than that of the free standing crystal krypton. The premixed gas samples were deposited at 17 K, through a pair of solenoid valves, with a dead volume of 2 cm^3 and at a back pressure of 200 Torr. Either sapphire, or rhodium-coated cop-

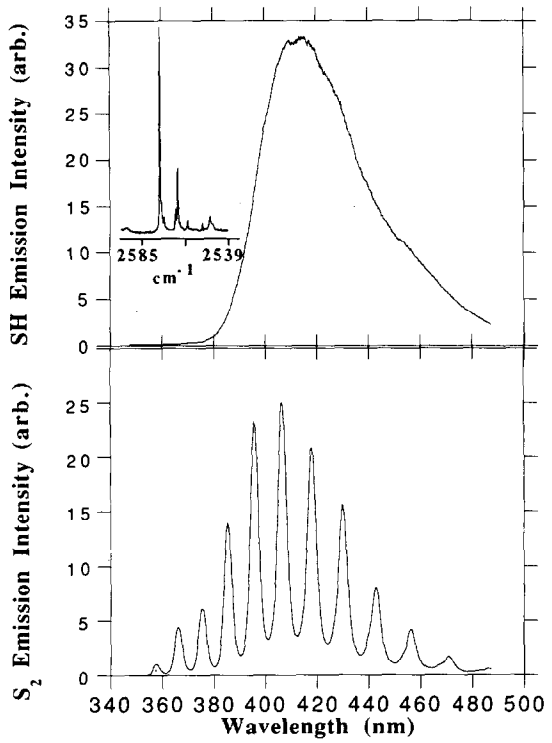

Fig. 1. Top panel: SH(A→X) emission spectrum in free standing crystal krypton, from a sample with nominal H_2S:Kr ratio of 1:10000. Also shown is the infrared absorption spectrum of $(H_2S)_2$. The absorption at 2566 cm^{-1} is assigned to the H-bonded stretch while the line at 2575.5 cm^{-1} is assigned to the free SH stretch (see ref. [30]). Lower panel: S_2(B→X) emission spectrum obtained after UV irradiation of the crystal.

per were used as substrates. H_2S of 99.5% purity and Kr of 99.999% purity were used without further purification. Passivation of the metal manifold was necessary to retain the H_2S concentration in the sample.

A variety of lasers were used as dissociation sources: the doubled output of an excimer pumped dye laser (Lambda Physik EMG101/FL2002) was used in the spectral range between 255 and 217 nm; an ArF excimer laser (Lambda EMG 201) for dissociation at 193 nm; at the longest wavelength of the measurements, at 266 nm, due to the very weak absorption of H_2S ($\sigma_{gas}=1.44\times10^{-20}$ cm^2) the fourth harmonic of a mode-locked YAG laser was used to provide the necessary photon flux. The SH dissociation product was probed with an excimer pumped dye laser (Lambda EMG201/FL3002). The probe laser excites the SH (A, $v=0$)←(X, $v=0$) transition at 332 nm [22]. The Stokes shifted SH(0,0) emission at 417 nm was collected and dispersed through a 0.75 meter monochromator (SPEX 1702) and detected with a photomultiplier tube (Hamamatsu 758) using an averaging digital oscilloscope (Tektronix 2430). Care is taken to probe an area smaller than that of the dissociation: typically, 20 μJ pulses over an area of 3×10^{-3} cm^2 is used to probe. The dissociation laser energy is measured by a factory-calibrated Joulemeter (Gentec ED 100), and the beam area is measured by scanning a 50 μm pinhole in the sample plane. The photoproduction of S atoms was verified by thermoluminescence – after completion of experiments, when the solid is warmed to above 30 K, thermoluminescence from S_2 is observed (see emission spectrum in fig. 1).

3. Results and discussion

A typical growth curve in SH fluorescence as a function of irradiation time, is shown in fig. 2. The growth curve is well fit by a single exponential, as indicated in fig. 2. It was verified that in the power range of measurements the photodissociation is single photon induced. As mentioned above, in addition to the SH+H channel, there is clear evidence of S atom formation in this photodissociation process. As such, photoexcitation fo the H_2S impurity in Kr,

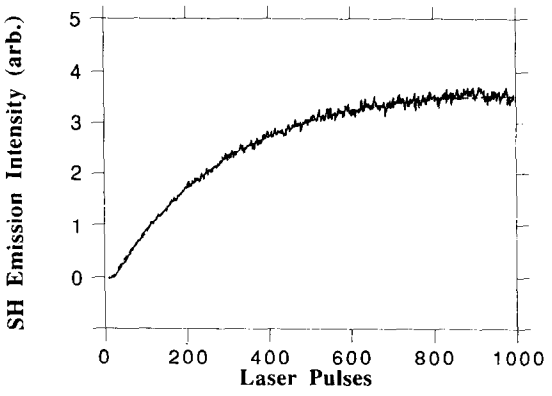

Fig. 2. Growth curve of SH(A→X) emission, from a matrix of H_2S:Kr ratio of 1:10000, irradiated at 225 nm, at a laser intensity of 8.4 mJ/cm^2. The emission is monitored by exciting the same volume at 332 nm, on the (0, 0) transition of SH(A←X).

$$H_2S+h\nu\rightarrow H_2S^*, \quad \sigma(\lambda), \tag{1}$$

may result in one of three outcomes,

$$H_2S^*\rightarrow H_2S, \quad p_1, \tag{2a}$$

$$H_2S^*\rightarrow H+SH, \quad p_2, \tag{2b}$$

$$H_2S^*\rightarrow S+H_2, \quad p_3, \tag{2c}$$

with probabilities, p_1, p_2, and p_3 of recombination, cage exit of H atom, or cage-induced reaction to form S atoms, respectively. The thermodynamic threshold for the latter channel depends on the electronic state of S atom: 3.02 eV for $S(^3P)$, 4.17 eV for $S(^1D)$ and 5.77 eV for $S(^1S)$ [#1]. The time evolution of the SH fragment, which is monitored in these experiments, is then given as:

$$SH(t)=\frac{[H_2S]_0 p_2}{p_2+p_3}\,[1-\exp(-\sigma\phi lt)], \tag{3a}$$

where

$$\phi=\frac{p_2+p_3}{p_1+p_2+p_3}, \tag{3b}$$

in which I is the photon flux, and t the irradiation time. The product $\sigma\phi$, the total photodissociation cross section of H_2S, is directly obtained from the exponential fits to the data. These are illustrated in fig. 3b. The data span a range of over three orders of magnitude. To extract the photodissociation quantum yield, ϕ, the absorption cross sections are needed. We have used both the gas-phase absorption cross sections, and those derived from the absorption measurements in crystal Kr. The latter data are used after normalization to the gas-phase curve, by simply matching the end points of the spectra, see fig. 3a. This procedure is mandated by the fact that the absolute number density of the H_2S in the crystalline sample is not known. As can be seen, the absorption profile of H_2S in its red wing is quite similar to that of the gas phase. However, due to the fact that a reliable absolute number density in Kr is not available, the derived quantum yields could in principle be off by a proportionality constant which is wavelength independent. A second source of error in absolute quantum yields is introduced by the fact that we do not take scattering losses into account. The matrices prepared in the present studies are consistently optically scattering. The absorption cross sections, photodissociation cross sections, and extracted photodissociation quantum yields, are collected in table 1.

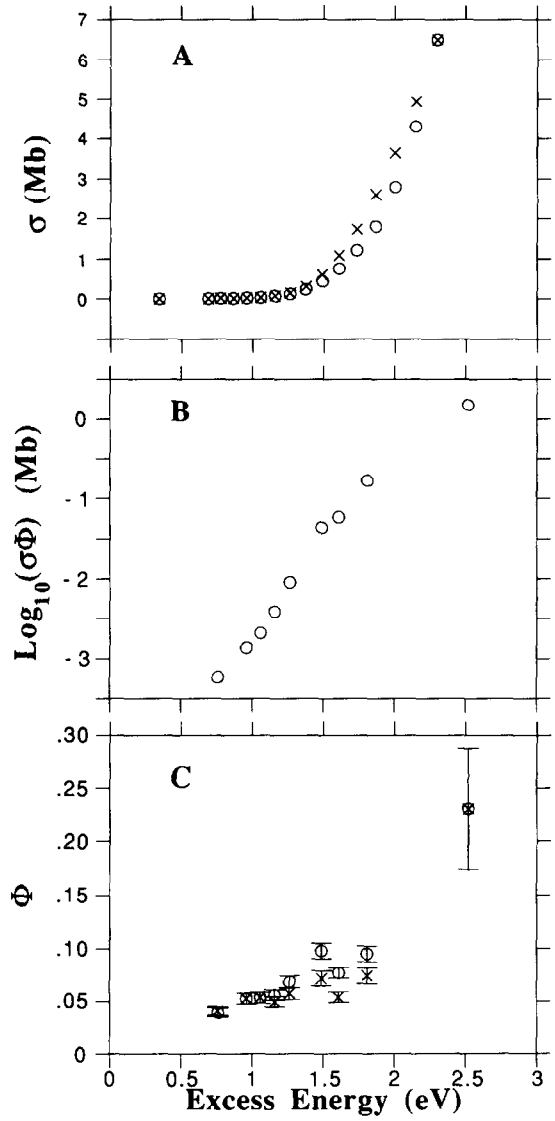

Fig. 3. (a) Gas-phase absorption cross section of H_2S (○) recorded at 10.7 Torr in a cell of 5 cm pathlength; and the absorption spectrum in crystal Kr (×) after normalizing the end points to the gas-phase values. (b) Photodissociation cross sections, as obtained from growth curves. (c) Photodissociation, quantum yields as referenced to gas (○) and solid Kr (×) absorption cross sections.

[#1] Values used are from ref. [20], except for the bond energy of SH for which the value of 3.62 eV is used according to ref. [23].

Table 1
Experimental data: excitation wavelength (λ), excess energy (E_{excess}), absorption cross sections (σ), photodissociation cross section ($\sigma\phi$), and dissociation quantum yields (ϕ) based on gas and solid-state absorption cross sections

λ (nm)	E_{excess} [a] (eV)	σ_{gas} [b] (Mb)	σ_{Kr} [c] (Mb)	$\sigma\phi$ (cm^2)	ϕ_g [d]	ϕ_{Kr} [e]
193	2.52	6.50	6.50	1.50×10^{-18}	0.230	0.230
217	1.81	1.75	2.24	1.67×10^{-19}	0.074	0.058
225	1.61	0.763	1.09	5.90×10^{-20}	0.054	0.038
230	1.49	0.445	0.606	4.37×10^{-20}	0.072	0.052
240	1.26	0.130	0.156	9.00×10^{-21}	0.057	0.048
245	1.16	0.069	0.078	3.90×10^{-21}	0.050	0.044
250	1.06	0.039	0.039	2.10×10^{-21}	0.054	0.054
255	0.96	0.026	0.026	1.38×10^{-21}	0.053	0.053
266	0.76	0.014	0.014	5.96×10^{-22}	0.041	0.041

[a] $E_{excess}=h\nu-D_0$; $D_0=3.91$ eV.
[b] $Mb=10^{-18}$ cm^2.
[c] Absorption cross sections in kr, with end points normalized to the gas-phase values.
[d] Quantum yields based on σ_{gas}.
[e] Quantum yields based on σ_{Kr}.

The same data are presented graphically in fig. 3. A systematic deviation, as large as 25%, exists between the quantum yields obtained from the gas phase, and the normalized solid-state absorptions. The deviation could be made much smaller by a different choice of points for normalization, however, this would not significantly change the conclusions to be presented. The indicated error bars are mainly determined by the uncertainty in the dissociation laser intensity. The large error bar associated with the measurement at 193 nm, is due to the shot-to-shot instability of the particular laser used.

The photodissociation quantum yields in fig. 3 are presented as a function of excess energy – energy above the dissociation limit of H_2S, $E=h\nu-D_e$ and $D_e=3.91$ eV [16]. In the 0.75–2 eV range of excess energies, the quantum yields show a linear dependence, and within the errors of the measurement can be extrapolated to zero intercept. This is the main result that we wish to convey with this paper.

The observed excess energy dependence of photodissociation quantum yields is in sharp contrast with the equivalent measurements of H_2O dissociation in rare-gas matrices in which a sharp energetic threshold for dissociation probabilities is extracted [6–9]. In the case of H_2O/Kr, the threshold occurs at an excess energy of 1.5 eV. The threshold is ascribed to the potential energy barrier for cage exit – the energy for passage of the H atom through the D_{3h} window formed by three mutual nearest-neighbor Kr atoms. The observation of such a threshold, would clearly imply that the molecular dissociation is determined by the sudden cage exit of the H atom over a barrier which is potential in nature, i.e. without extensive thermalization.

Given the similarity of systems, such a dramatic difference in behavior was not expected. Note, what is measured in these experiments is the overall photodissociation probability of the parent molecule. A process, which could be determined by either the cage exit of the H atom, eq. (2b), or by the in-cage reaction of photofragments, eq. (2c). Initial estimates of the branching ratios indicate that both channels are equally important in the measured range of energies. If the cage exit of the H photofragment is the dominant dissociation channel, then the lack of an energetic threshold in dissociation probabilities would be consistent with the scenario of delayed exit. On the other hand, if the dissociation channel is dominated by the $S+H_2$ channel, one would be forced to conclude that the H atom exit is not sudden. In either case, our data are more consistent with the molecular dynamics simulations, which predicted a delayed exit of the H photofragment: the hot H atom loses most of its initial kinetic energy on the time scale of 100–200 fs by collisions with cage at-

oms, and exists the "hot" cage several picoseconds after dissociation [1].

The source of disagreement between the present data and those on H_2O if not experimental in nature, then could point to an important difference in the dynamics of these two molecules. Two independent measurements are needed for the extraction of dissociation quantum yields, the photodissociation cross section, $\sigma\phi$, and the molecular absorption cross section, σ. Measurement of absolute absorption cross sections in the solid state is usually the more difficult task. This task is complicated by uncertainties in absolute number densities, difficulty in accounting for scattering background contributions to characteristically broad bound-to-repulsive absorptions, and potential interferences from impurity and aggregate absorptions. In the present, we measured the absorption profile in the spectral range of interest, in a free standing crystal of high optical quality, with a dopant dilution of order 1:100000. Due to the uncertainty in the number density of dopants, we then relied on normalizing the profile to the gas-phase spectrum of H_2S. Only because the normalized spectra are quite similar, is this procedure acceptable. Nevertheless, all of our measurements are subject to an uncertainty in absolute quantum yields, which however is a constant throughout the spectral range of measurements. In the case of H_2O, strongly shifted absolute absorption spectra are recorded in different matrices. In addition to spectral shifts, the development of a red wing is noted in all samples. it is in the spectral range of the red wing that dissociation thresholds are observed. If these red wings, the origin of which is not clear, were due to absorbers other than isolated H_2O monomers, then a false threshold would be extracted from the photodissociation cross sections. This hypothesis could in principle be tested by dilution experiments.

The observed difference in behavior between H_2O and H_2S photodissociation could be more fundamental in nature. The fact that in H_2O the first absorption is purely dissociative, while in H_2S mixed states are accessed, could affect the dissociation dynamics in a profound manner. In the case of H_2S, at an excess energy of 1.5 eV, we estimate nearly equal contributions to dissociation via the SH+H and $S+H_2$ channels. This channel has not been reported in the H_2O studies, even though it should have been accessible in the energy range of the studies. If indeed the $O+H_2$ channel is not important in the solid state-dissociation of H_2O, then it would be concluded that the observed dynamics are more strongly affected by the molecular electronic surface, as opposed to the pure mechanics of H atom cage exit.

4. Conclusions

The photodissociation probability of H_2S isolated in matrix Kr shows a mild, linear dependence on excess energy. The dissociation proceeds via two channels: cage exit of H and in-cage reaction between SH and H fragments to yield S atoms. Based on the total dissociation probabilities as a function of excess energy, it is possible to assert that the data are incongruent with the sudden cage exit model suggested by the recent experimental studies of H_2O dissociation in rare-gas matrices [6–9]. Our data are consistent with the delayed cage exit of H photofragments suggested by earlier molecular dynamics simulations, and experimental studies on HI dissociation in Xe [1–4]. The possible sources of disagreement between the H_2S and H_2O data are suggested to be either experimental in nature, mainly associated with the determination of absorption spectra in matrices, or due to differences in electronic surfaces accessed in these two systems.

To date, photodissociation studies in solids have mainly emphasized the nuclear dynamics of photofragments on a single electronic surface, e.g. delayed versus sudden cage exit. The control of dynamics by electronic degrees of freedom has for the most part been ignored, despite the fact that dissociation probabilities are determined by cage exit versus recombination, therefore minimally a two-surface problem. In the case of H_2S, the presence of several reactive channels could enable the determination of the interplay between electronic and nuclear degrees of freedom. Measurements of branching ratios between these different channels are now in progress in our laboratory. Theoretical simulations of many-body, multisurface dynamics, will be necessary for the interpretation of such data, and in general for progress in the field of condensed phase reactive dynamics.

Acknowledgement

This research was supported by the US Air Force Phillips Laboratory under contract S04611-90-K-0035, and by a grant from the National Science Foundation, ECS-8914321.

References

[1] R. Alimi, R.B. Gerber and V.A. Apkarian, J. Chem. Phys. 89 (1988) 174.
[2] R.B. Gerber and R. Alimi, Chem. Phys. Letters 173 (1990) 393.
[3] W.G. Lawrence, F. Okada and V.A. Apkarian, Chem. Phys. Letters 150 (1988) 339.
[4] W.G. Lawrence, Ph.D. Thesis (University of California, Irvine, 1992).
[5] H. Kunttu, J. Seetula, M. Rasanen and V.A. Apkarian, J. Chem. Phys. 96 (1992) 5630.
[6] R. Schriever, M. Chergui, H. Kunz, V. Stepanenko and N. Schwentner, Chem. Phys. 91 (1989) 4128.
[7] R. Schriever, M. Chergui, O. Unal, N. Schwentner and V. Stepanenko, J. Chem. Phys. 93 (1990) 3245.
[8] R. Schriever, M. Chergui and N. Schwentner, J. Chem. Phys. 93 (1990) 9206.
[9] N. Schwentner, J. Mol. Struct. 222 (1990) 151.
[10] R. Schriever, M. Chergui and N. Schwentner, J. Phys. Chem. 95 (1991) 6124.
[11] N. Blake and V.A. Apkarian, manuscript in preparation.
[12] B. Heumann, R. Duren and R. Schinke, Chem. Phys. Letters 180 (1991) 583.
[13] K. Weide, V. Staemmler and R. Schinke, J. Chem. Phys. 93 (1990) 861.
[14] F. Flouquet, Chem. Phys. 13 (1976) 257.
[15] K.C. Kulander, Chem. Phys. Letters 103 (1984) 373.
[16] R.N. Dixon, C.C. Marston and G.G. Balint-Kurti, J. Chem. Phys. 93 (1990) 6520.
[17] W.J. Hawkins and P.L. Houston, J. Chem. Phys. 73 (1980) 297; 76 (1982) 729.
[18] R.J. Brudzynski, R.J. Sension and B. Hudson, Chem. Phys. Letters 165 (1990) 487.
[19] X. Xie, L. Schneider, H. Wallmeier, R. Boettner, K.H. Welge and M.N.R. Ashfold, J. Chem. Phys. 92 (1990) 1608.
[20] L. Schneider, W. Meier, K.H. Welge, M.N.R. Ashfold and C.M. Western, J. Chem. Phys. 92 (1990) 7027.
[21] M.D. Person, K.Q. Lao, B.J. Eckholm and L.J. Butler, J. Chem. Phys. 91 (1989) 812.
[22] G.N.A. Van Veen, K.A. Mohamed, T. Baller and A.E. De Vries, Chem. Phys. 74 (1983) 261.
[23] R.E. Continetti, B.A. Balko and Y.T. Lee, Chem. Phys. Letters 182 (1991) 400.
[24] V. Engel, R. Schinke and V. Staemmler, J. Chem. Phys. 88 (1988) 129;
P. Anderson and R. Schinke, Molecular photodissociation dynamics, eds. M.N.R. Ashfold and J.E. Baggot (Royal Chem. Soc., London, 1987).
[25] J. Franck and E. Rabinowitch, Trans. Faraday Soc. 30 (1934) 120; 32 (1936) 547, 1381.
[26] D. Imre, J. Zoval and V.A. Apkarian, manuscript in preparation.
[27] W.G. Lawrence and V.A. Apkarian, J. Chem. Phys., in press.
[28] V.E. Bondybey and J.H. English, J. Chem. Phys. 72 (1980) 3113.
[29] L. Brewer and G.D. Brabson, J. Chem. Phys. 44 (1966) 3274.
[30] E. Woodbridge, T.L. Tso, M. McGrath, W. Hehre and E.K.C. Lee, J. Chem. Phys. 85 (1986) 6991.